

## Evaluation of satellite estimates of downward shortwave radiation over the Tibetan Plateau

Kun Yang,<sup>1</sup> Rachel T. Pinker,<sup>2</sup> Yaoming Ma,<sup>1</sup> Toshio Koike,<sup>3</sup> Margaret M. Wonsick,<sup>2</sup> Stephen J. Cox,<sup>4</sup> Yuanhong Zhang,<sup>5</sup> and Paul Stackhouse<sup>6</sup>

Received 19 December 2007; revised 25 May 2008; accepted 11 June 2008; published 9 September 2008.

[1] The state-of-the-art satellite products of downward shortwave radiation over the Tibetan Plateau against ground observations are evaluated in this study. The satellite products include the International Satellite Cloud Climatology Project-Flux Data (ISCCP-FD) as produced at the NASA Goddard Institute for Space Studies (GISS) from the ISCCP D1 data, the Global Energy and Water Cycle Experiment-Surface Radiation Budget (GEWEX-SRB) results as derived at the NASA Langley Research Center (LaRC) from the ISCCP DX data, and a University of Maryland product derived with a modified version of the University of Maryland Surface Radiation Budget (UMD-SRB) model as implemented with METEOSAT-5 observations. These products are at different spatial and temporal resolutions, and the evaluation is performed at their native resolutions. Comparisons indicate that, in this region of great variation in elevation, using hourly, spatially homogeneous, and high resolution satellite data (UMD-SRB) compares more favorably with surface measurements than products that use three hourly, sparse subsamples at coarse resolutions (ISCCP-FD and GEWEX-SRB). Discrepancies among the satellite products are usually larger in highly variable terrain (such as in the Himalayas region) and smaller for nonvariable terrain (such as in the central Plateau). This suggests that errors of satellite products are spatially dependent over the Tibet. Therefore caution needs to be exercised when extending comparison results based on limited in situ data from accessible sites to the entire Plateau. Attention should be also given to the quality of input parameters besides cloud properties, as there are large discrepancies among the satellite products for clear-sky radiation.

**Citation:** Yang, K., R. T. Pinker, Y. Ma, T. Koike, M. M. Wonsick, S. J. Cox, Y. Zhang, and P. Stackhouse (2008), Evaluation of satellite estimates of downward shortwave radiation over the Tibetan Plateau, *J. Geophys. Res.*, 113, D17204, doi:10.1029/2007JD009736.

### 1. Introduction

[2] The protruding nature of the Tibetan Plateau affects the migration and the temporal variability of the Asian Monsoon system through its prominent orography and thermal dynamics [Yeh and Gao, 1979; Yanai *et al.*, 1992; Wu *et al.*, 2007]. It has been recognized that the plateau is a large heat source for the Northern Hemisphere [Yeh *et al.*, 1957; Flohn, 1957]. Therefore the quantification of the water and energy cycles is an important issue in studies of the Tibetan hydrometeorology and Asian Monsoon. Due to

the lack of observations over the Tibet, current studies of quantitative type show large uncertainties [Chen *et al.*, 2003]. Satellite remote sensing is a promising approach to enhance our understanding of the water and energy cycles in this region [Y. Ma *et al.*, 2007]. Yang *et al.* [2007] are in the process of developing a land data assimilation system, which assimilates satellite microwave data to produce reliable continuous land heat fluxes to better understand the surface water and energy budgets. Radiative fluxes are part of this budget and therefore the quality of available information needs to be established. In the Tibet region, the mean surface elevation is above 4000 m MSL. The peculiar plateau conditions (low air mass, low aerosol concentration, low precipitable water, and low ozone concentration) result in high values of downward shortwave radiation (SWD). Observations show that the downward shortwave radiation over the Tibet can reach  $1200 \text{ W m}^{-2}$  or more at local noon in summer [Ma *et al.*, 2005], which is much higher than that over sea level along the same latitude. In addition to the high elevation, the plateau has complex terrain, with several west–east running high mountains and many hills. The complex terrain can affect solar radiation in direct and

<sup>1</sup>Institute of Tibetan Plateau Research, Chinese Academy of Sciences, Beijing, China.

<sup>2</sup>Department of Atmospheric and Oceanic Science, University of Maryland, College Park, Maryland, USA.

<sup>3</sup>Department of Civil Engineering, University of Tokyo, Tokyo, Japan.

<sup>4</sup>Analytical Services and Materials, Inc., One Enterprise Parkway, Hampton, Virginia, USA.

<sup>5</sup>Columbia University at NASA GISS, New York, New York, USA.

<sup>6</sup>NASA Langley Research Center, Hampton, Virginia, USA.

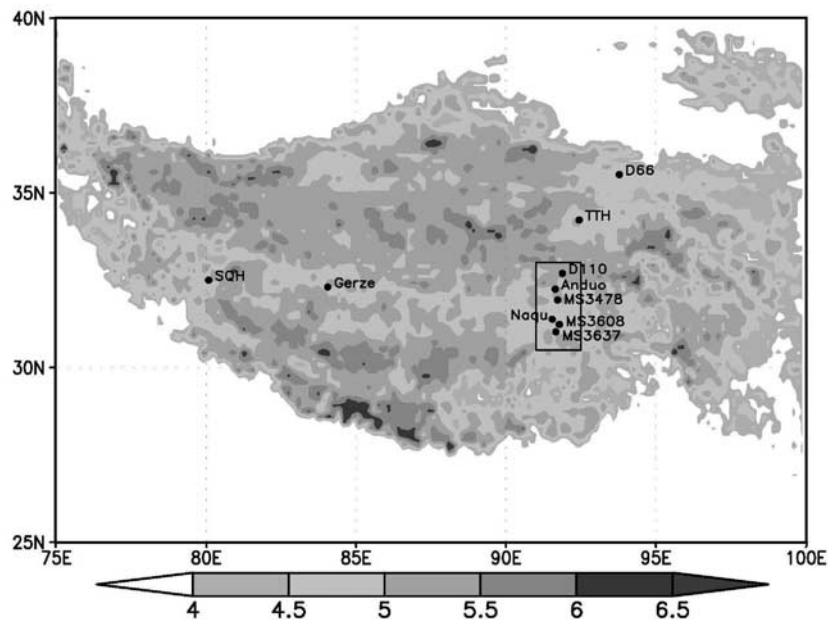


**Figure 1.** Map of GAME-Tibet experiment, IOP 1998. Gray bar represents elevation in kilometers. Ten radiation sites are marked with solid dots; six sites were deployed within the 91–92.5°E, 30.5–33°N region. SQH and TTH are the abbreviation of Shiquanhe and Tuotuohe sites of GAME-Tibet experiments, respectively.

indirect ways. Direct effects include shading by mountain peaks and multiple scattering related to elevation-dependent snow cover. Indirect effects include convective orographic clouds and redistribution of precipitation over mountains and valleys by large-scale and local-scale diurnally changing winds induced by the complex terrain [Ku wagata *et al.*, 2001; Kurosaki and Kimura, 2002]. As shown in Liou *et al.* [2007], average surface solar flux over a region with complex topography can deviate from a smooth surface by as much as 10–50 W m<sup>-2</sup>, and the anomalies of solar flux can be as large as 600 W m<sup>-2</sup>. Due to the altitudinal dependence of the downward shortwave radiation, caution needs to be exercised when applying current satellite products to the plateau region. Most of the evaluations of these products have been performed at low elevation areas where good accuracy has been demonstrated. Therefore ground observations over the Tibetan Plateau can be used as a benchmark for evaluation of satellite algorithms at high elevations [Yang *et al.*, 2006a].

[3] In this study, we consolidated in situ data and several state-of-the-art satellite products for the Tibet region, and attempted to evaluate the satellite products against surface observations. It is an extension of the work of Yang *et al.* [2006a], in which a preliminary assessment of selected satellite products was conducted. In this study, we added one improved version of earlier products, a new version of a high spatial and temporal resolution product, and focused on spatial variability of the downward shortwave radiation. In situ data and satellite data are introduced in section 2. In section 3 compared are satellite products with in situ data. In section 4 analyzed is the spatial variability of the downward shortwave radiation. In section 5, discussion is extended to the entire plateau to learn about the role of the terrain on the discrepancies among the products and the role of terrain

variability in the retrievals. Concluding remarks are given in section 6.

## 2. Data

### 2.1. In Situ Data

[4] In situ data were collected under the GEWEX Asian Monsoon Experiments-Tibet (GAME-Tibet) during an intensive observing period (IOP, May–September 1998) [Koike *et al.*, 1999]. Figure 1 shows the observing network and Table 1 shows basic information on 10 sites. The elevation of all stations was above 4000 m MSL. To achieve representativeness, the sites were deployed along a north–south and a west–east transects and more than half of them were placed within a mesoscale area (30.5–33°N, 91–92.5°E). Several types of pyronometers were used in GAME-Tibet, such as VAISALA CM6B (compliant with ISO 9060 first class specification), Kipp-Zonen CM-21, and CNR1 (compliant with ISO 9060 second class specification). Data were sampled every second and the average of each 10, 30, or 60 minutes period was recorded. Calibration coefficients are provided by manufacturers. Recent studies have found that systematic errors in radiation measurements are not uncommon [Kato *et al.*, 1997; Dutton *et al.*, 2001], the GAME-Tibet radiation data set is still the most reliable one for the elevated region. For the MS3608 site, the measured values for many hours are much higher than the clear-sky values estimated by a high-accuracy model [Yang *et al.*, 2006b], and frequently higher than the solar constant. While it is possible to measure values higher than the solar constant (up to 10% more due to reflection from clouds), the high frequencies of such values at the MS3608 site is unexpected.

**Table 1.** GAME-Tibet Shortwave Radiation Observing Sites

No.	Station	In situ			Record Interval (minutes)	Data Length (day)
		Altitude (m)	Latitude (°N)	Longitude (°E)		
1	SQH	4282	32.5	80.08	60	81
2	Gerze	4420	32.3	84.05	60	92
3	MS3637	4820	31.02	91.66	30	74
4	MS3608	4610	31.23	91.78	10	64
5	Naqu	4496	31.38	91.54	30	77
6	MS3478	5063	31.93	91.72	30	78
7	Anduo	4700	32.24	91.64	30	77
8	D110	5070	32.69	91.88	10	35
9	TTH	4535	34.22	92.44	10	83
10	D66	4600	35.52	93.78	10	84

## 2.2. Satellite Data

[5] Satellite products of surface radiation from three research teams were used in this study; basic information on the algorithms and resolution is given in Table 2. Three products come from NASA LaRC. Two are based on the GEWEX-SRB approach [Stackhouse *et al.*, 2004] as driven with the ISCCP DX data gridded at  $1^\circ$  spatial resolution using V2.5 and V2.81 of the inference scheme. The GEWEX-SRB V2.5 product has been previously evaluated [Yang *et al.*, 2006a] and is included here for completeness. A major difference between V2.5 and V2.81 is that the lookup tables in the radiative transfer code of V2.5 does not account for elevation and its effect on Rayleigh scattering while in V2.81 this effect was included. The GEWEX-SRB approach use cloud cover and radiances from the ISCCP-DX nominal 30-km pixels within each  $1^\circ \times 1^\circ$  cell [Cox *et al.*, 2006]. The third product is from a quality-check algorithm (GEWEX-QCSW V2.5) based on Gupta *et al.* [2001] as driven with the same data. The fourth product is the newest version from GISS [Zhang *et al.*, 2004] and is based on the ISCCP D1 data at 280-km resolution (ISCCP-FD). Used are cloud cover, cloud top temperature, optical thickness, and cloud phase based on 15 cloud types in the ISCCP-D1 280-km equal-area grid with climatologies for cloud particle size and vertical structure [Zhang *et al.*, 2004; Rossow and Schiffer, 1999]. The fifth product is from the University of Maryland (UMD). It is based on a modified version of the UMD Surface Radiation Budget (UMD-SRB) as described in Y.-T. Ma *et al.* [2007]. The model was implemented with the high resolution observations from METEOSAT-5. The cloud detection for METEOSAT-5 is based on a methodology described in Li *et al.* [2007] for GOES-8 as subsequently modified for METEOSAT-5. Initial information on aerosols is taken from H. Liu *et al.* [2005]. In support of the Indian Ocean Experiment (INDOEX) [Ramanathan *et al.*, 2001], METEOSAT-5 was moved to  $63^\circ\text{E}$  longitude, and continuous operational coverage of the area began in July 1998. This unique data set provides an opportunity to supplement current information on cloud-related parameters in this monsoon-dominated region. The Coordinated Enhanced Observing Period (CEOP) [Koike, 2004] recognizes the importance of the monsoon systems, and a primary goal of this program is to produce a long observational record of water and energy parameters to support monsoon research. In response to CEOP objectives an attempt has been made to derive high resolution cloud parameters and shortwave radiative fluxes

from METEOSAT-5 satellite observations. Specifically, algorithms to derive clouds [Li *et al.*, 2007] and shortwave radiative fluxes [Pinker *et al.*, 2003] from GOES-8 observations over the United States have been adapted to process METEOSAT-5 data over this region. Visible ( $0.75\ \mu\text{m}$ ) and infrared ( $11.5\ \mu\text{m}$ ) data collected by the satellite at 5-km resolution are used for clear/cloudy sky determination, with final results projected onto a  $0.125^\circ$  latitude/longitude grid. The cloud detection algorithm requires knowledge of snow conditions to prevent misrepresentation of snow or ice as clouds. Snow cover information is obtained from the Interactive Multisensor Snow and Ice Mapping System (IMS) data set, a manually developed global snow mask produced at the National Centers for Environmental Prediction (NCEP) [Ramsay, 1998]. Precipitable water is needed for the calculation of cloud optical depth, and such information is extracted from the NCEP Reanalysis II, which is documented at <http://www.cdc.noaa.gov/cdc/reanalysis/reanalysis.shtml>.

[6] Attention should be paid to the differences in the sampling of cloud properties. In the GEWEX-SRB and in QCSW the basic observations used are the ISCCP DX products which are based on single 4 by 8 km pixels randomly subsampled at 30-km resolution every 3 hours. These are aggregated to a  $1^\circ$  grid. The ISCCP D1 product is used to derive the ISCCP-FD fluxes; it represents a mean value of DX pixels in each 280-km equal-area grid. The UMD-SRB model uses hourly METEOSAT-5 5-km pixels without sampling.

[7] Surface radiation components from GEWEX-SRB and ISCCP-FD have been widely assessed at numerous locations over the globe by data developers [Cox *et al.*, 2006; Zhang *et al.*, 2004] and independently [J. Liu *et al.*, 2005; Xia *et al.*, 2006; Raschke *et al.*, 2006]. The UMD-SRB model has been evaluated against high-quality data from the Surface Radiation Budget Network (SURFRAD) and the Baseline Surface Radiation Network (BSRN) [Liu and Pinker, 2008], where UMD-SRB model was implemented with the ISCCP D1 data.

[8] The UMD-SRB product used in this study is a relatively new product for highlands and can benefit from additional evaluations.

[9] The period of July, August, September 1998 was selected for evaluation since high-quality ground observations and all the satellite products are available. Because of occasional unavailability of satellite scenes, some data are missing in the UMD-SRB product. A gap filling was performed by assuming a daily mean transmittance of solar radiation. This interpolation may affect the evaluation results, in particular, at the shorter timescales.

[10] These satellite products are of different temporal resolutions, and initially, the evaluation is performed at

**Table 2.** Basic Information of Satellite Products of Downward Shortwave Radiation

Products	Spatial Resolution	Temporal Resolution	Algorithm
GEWEX-SRB V2.5	$1.0^\circ$	3 hr	Pinker and Laszlo [1992]
GEWEX-SRB V2.81	$1.0^\circ$	3 hr	Modified Pinker and Laszlo [1992]
GEWEX-QCSW V2.5	$1.0^\circ$	daily	Gupta <i>et al.</i> [2001]
ISCCP-FD	$2.5^\circ$	3 hr	Zhang <i>et al.</i> [1995, 2004]
UMD-SRB	$0.125^\circ$	1 hr	See the text

**Table 3.** Mean Bias Errors (MBE) of Satellite Products and Standard Deviation (SD) of the Differences Between Observed and Satellite Downward Shortwave Radiation ( $\text{W m}^{-2}$ ) at GAME-Tibet Radiation Sites for July–September 1998<sup>a</sup>

Site	SQH	Gerze	MS3637	Naqu	MS3478	Anduo	D110	TTH	D66	Ave
<i>Observed Mean Value</i>										
	293.6	268.5	235.2	237.2	240.8	243.4	259.5	257.2	256.3	254.6
<i>Mean Bias Error</i>										
GEWEX V2.5	−37.4	−69.0	−45.2	−60.7	−42.7	−37.3	−62.4	−48.9	−39.6	−49.2
GEWEX V2.81	−10.2	−13.3	−15.5	−29.5	−12.9	−6.3	−32.2	−19.1	−9.4	−16.5
ISCCP-FD	−11.9	−16.7	−12.1	−10.3	−9.6	−17.1	−10.0	−15.7	−3.8	−11.9
UMD-SRB	−0.1	−14.5	12.7	−0.8	0.8	9.3	−3.1	−5.6	−6.7	−0.9
<i>Standard Deviation of the Differences Between 3-hr-mean Observation and Satellite Product</i>										
GEWEX V2.5	69.5	149.8	104.0	106.8	112.4	85.7	107.0	104.2	108.6	105.3
GEWEX V2.81	57.4	59.1	94.5	95.5	102.2	78.7	100.5	88.3	95.3	85.7
ISCCP-FD	83.6	77.9	89.1	83.3	99.2	101.7	102.9	83.9	90.6	90.2
UMD-SRB	82.3	83.0	95.8	89.4	109.2	87.6	101.3	91.3	89.3	92.1
<i>Standard Deviation of the Differences Between Daily-Mean Observation and Satellite Product</i>										
GEWEX V2.5	25.6	63.5	37.4	33.6	42.3	30.9	41.5	36.0	40.6	39.0
GEWEX V2.81	23.6	25.4	36.6	33.4	42.4	29.8	41.4	35.1	39.9	34.2
ISCCP-FD	41.9	34.4	34	30.3	45.7	45.5	42.3	34.6	37.8	38.5
UMD-SRB	25.8	32.2	45	36	35.7	30.3	31.8	25.3	29.5	32.4

<sup>a</sup>Ave, average values.

the native resolution of each product. Subsequently, we have aggregated the hourly estimates from the UMD-SRB model to 3-hourly values to facilitate comparison at same temporal scale. The difference between the two mean values (hourly and three hourly) is no more than  $1 \text{ W m}^{-2}$  at six sites and less than  $2.5 \text{ W m}^{-2}$  at all sites. The difference is small compared to the errors presented in Table 3, and thus do not affect the results of the evaluation.

### 3. Comparisons of Satellite and In Situ Data

[11] Table 3 shows the mean value of observed radiation, mean bias error (MBE) of satellite data and standard deviation (SD) of the differences between observation and satellite data for each site and the average. To maximize the use of observed data, statistical values in Table 3 were derived from 3-hourly data. GEWEX-QCSW V2.5 is not shown in this table since its temporal resolution is daily.

[12] Though the table shows that the biases are quite variable for the individual sites and months, systematic biases and tendencies may be identified. SWD fluxes from GEWEX-SRB V2.5 seem to underestimated the observations at all the observing sites. Biases for the individual sites are in the range of  $-30$  to  $-90 \text{ W m}^{-2}$  with an average value of  $-49 \text{ W m}^{-2}$  or  $-20\%$ . These errors are larger than reported in similar studies over flat terrain (about  $10 \text{ W m}^{-2}$  in Li *et al.* [1995],  $-5$  to  $-15 \text{ W m}^{-2}$  in Cox *et al.* [2006], and  $-9$  to  $28 \text{ W m}^{-2}$  in Xia *et al.* [2006]). In response to the earlier findings over the Tibet Plateau [Yang *et al.*, 2006a] the GEWEX-SRB algorithm was modified and resulted in V2.81. As evident from Table 3, the mean errors have been reduced by about  $30 \text{ W m}^{-2}$  at most of the sites, indicating the necessity to account for elevation in this complex region. The mean errors in GEWEX-SRB V2.81 product are about  $-16 \text{ W m}^{-2}$ , which is close to errors in other regions.

[13] At all the GAME-Tibet sites, ISCCP-FD underestimates the observed SWD. The high-resolution UMD-SRB product as implemented with the high resolution satellite observations from METEOSAT-5 is in close agree-

ment with the observations and its mean bias averaged over all the sites nearly vanishes (Table 3).

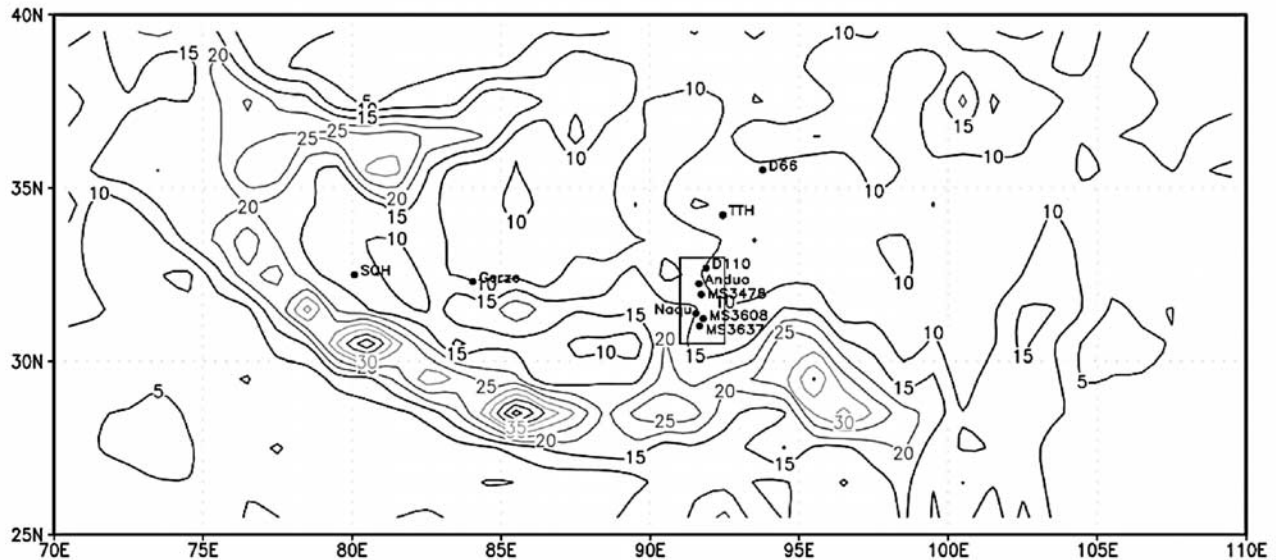
[14] SD values in Table 3 depend on temporal scale. While the UMD-SRB product has the smallest mean bias, the averaged standard deviation for the 3-hr-means are larger than GEWEX-SRB V2.81 and ISCCP-FD. This is probably related to cloud types in this region and the very windy conditions over the Plateau that affect the cloud movement. Convective clouds with small spatial scales (a few kilometers), which are called “popcorn” clouds by Chinese Scientists, appear most frequently over the Plateau [Yeh and Gao, 1979]. These convective clouds move quickly, due to the plateau windy conditions, and have short lifetime scales. Therefore the representativeness of pixels within a UMD-SRB grid can be well suited for instantaneous situations and long-term statistics but less so at hourly scale. Therefore it is plausible that the UMD-SRB model produced small MBE but high SD values for 3-hr-mean radiation. When the temporal scale of interest is extended from 3 hr to daily, UMD-SRB produced SD averages smaller than the others (see last four rows of Table 3).

**Table 4.** Standard Deviation of the Differences Between Observed and GEWEX-SRB/ISCCP-FD 3-Hourly SWD ( $\text{W m}^{-2}$ ) at the Mesoscale Experimental Sites Within a GEWEX-SRB or ISCCP-FD Grid<sup>a</sup>

GEWEX-SRB Grid					ISCCP-FD Grid	
Sites	SD		Sites	SD		
	V2.5	V2.81				
MS3637	104.0	94.5	MS3637	89.1		
Naqu	106.8	95.5	Naqu	83.3		
MS3478	112.4	102.2	MS3478	99.2		
			Anduo	101.7		
Grid-Ave	86.0	72.8	Grid-Ave	62.0		

<sup>a</sup>“Grid-Ave” is calculated from observed site-mean SWD and satellite SWD.

(a) Standard deviation of UMD-SRB SWD in 1.0-degree grids



(b) Standard deviation of UMD-SRB SWD in 2.5-degree grids

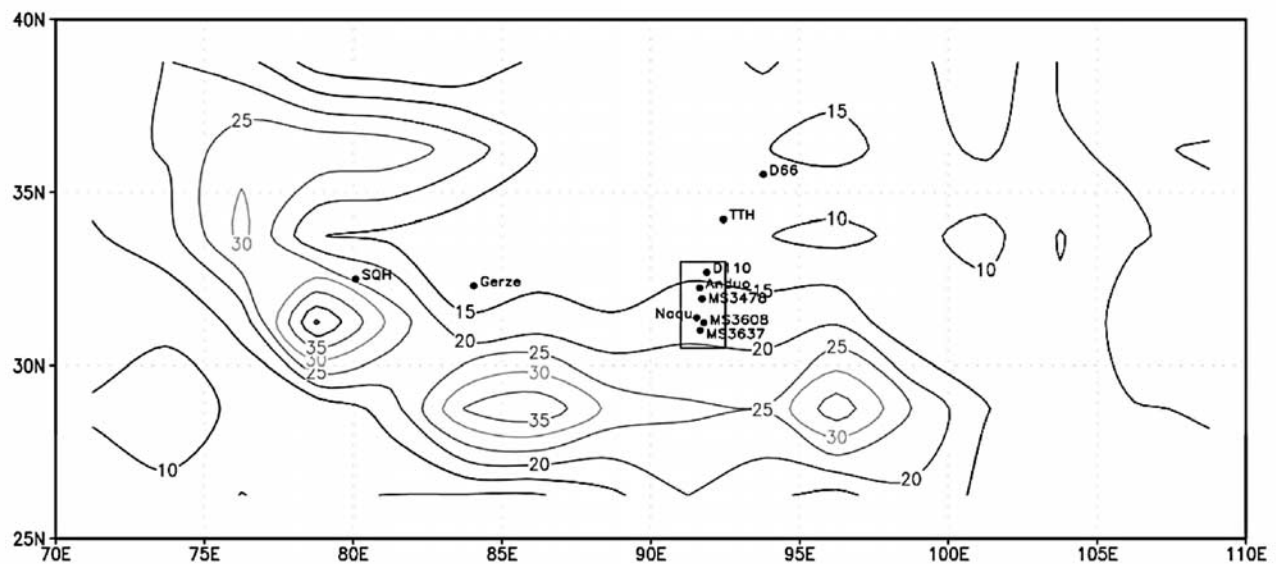


**Figure 2.** Standard deviation of UMD-SRB SWD in 1.0° grids (a) and 2.5° grids (b) in Tibet for the period of July–September 1998.

[15] In the mesoscale area, an ISCCP-FD grid includes sites MS3478, Naqu, Anduo, and MS3637. The bias of the ISCCP-FD SWD from the four-site mean is  $-13.0 \text{ W m}^{-2}$ . A GEWEX-SRB grid includes sites MS3478, Naqu, and MS3637. The bias of the GEWEX-SRB radiation from the three-site mean is  $-45.1 \text{ W m}^{-2}$  for V2.5 and  $-15.3 \text{ W m}^{-2}$  for V2.81. These mean biases are comparable to the biases from the individual sites. Table 4 shows the standard deviation of the differences between 3-hr-mean observations and satellite products for these sites. As seen, the standard deviation for the site-mean SWD within a GEWEX-SRB or ISCCP-FD grid (“Grid-Ave”) is much less than the ones for the individual sites. This result

suggests that comparing averaged observations with satellite data may reduce uncertainties significantly but not much for the mean bias of a satellite product in this mesoscale area.

#### 4. Spatial Variability of Shortwave Radiation

[16] The UMD-SRB is at much finer spatial resolution ( $\Delta x \sim 0.125^\circ$ ) than GEWEX-SRB ( $\Delta x \sim 1.0^\circ$ ) or ISCCP-FD ( $\Delta x \sim 2.5^\circ$ ). The UMD-SRB radiative flux over the Tibet is spatially variable (not shown). Therefore a question can be raised as to the impact of differences in spatial resolution on the accuracy of the estimates.

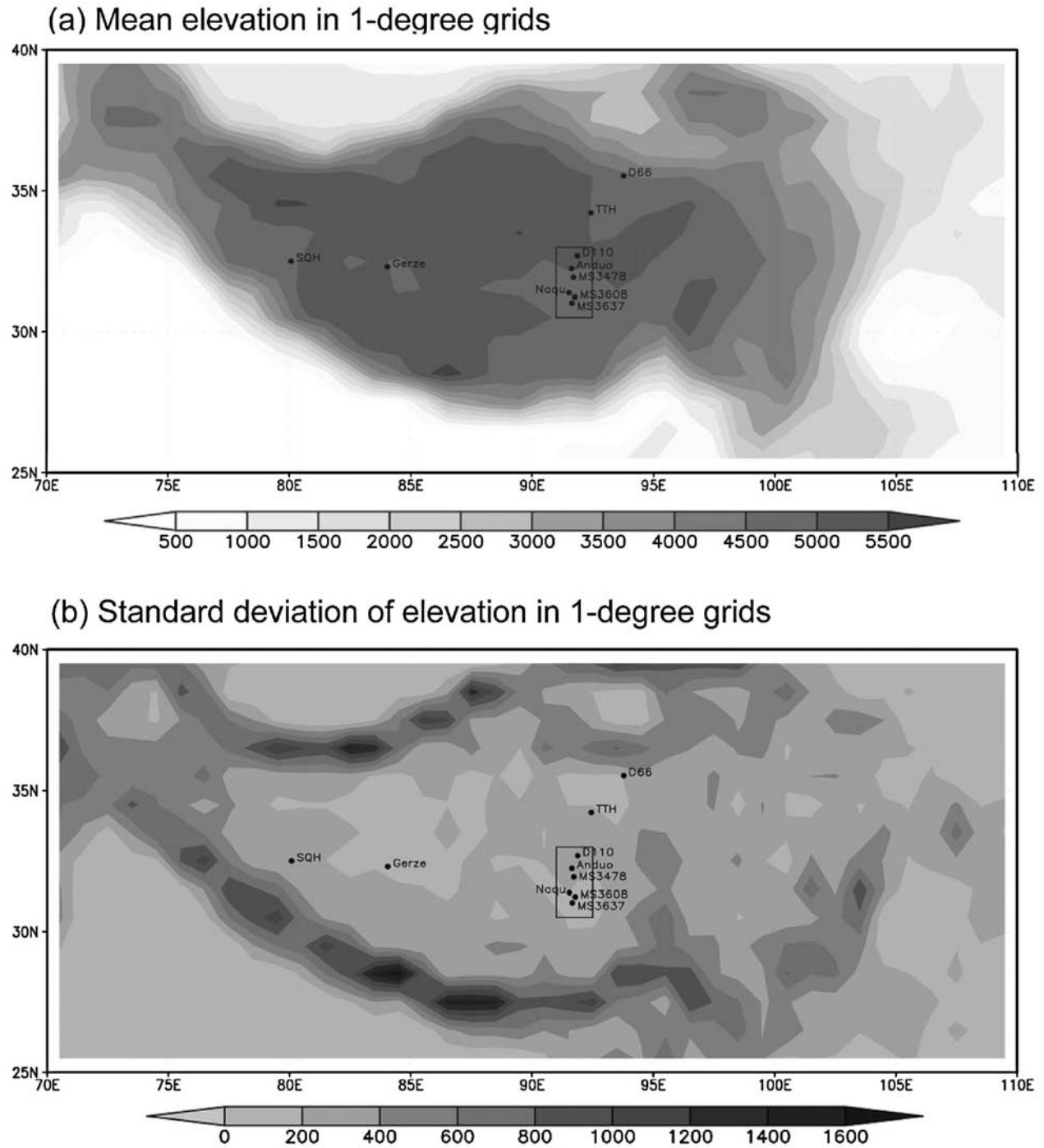


**Figure 3.** Mean elevation and standard deviation of elevation in  $1^\circ$  grids in the Tibet region. Data source: 5-minute DEM of National Geophysical Data Center TerrainBase Global DTM Version 1.0 (Lee W. Row, III and David Hastings).

[17] In response, we calculated the spatial variability of SWD that is measured by the standard deviation of SWD in a coarse grid. Figure 2 shows the standard deviation of three-monthly mean of UMD-SRB data at  $1.0^\circ$  (Figure 2a) and  $2.5^\circ$  grids (Figure 2b). The plateau topography and its variability at a  $1^\circ$  grid is shown in Figure 3. The central Plateau has higher mean elevation while the periphery of the Tibetan Plateau, particularly along Himalayas region, has

larger terrain variability. The UMD-SRB results show much larger spatial variability of SWD along the Himalayas and much smaller ones in the central plateau. This is not surprising, since SWD is affected significantly by elevation [Yang *et al.*, 2006b]. This correspondence suggests that the UMD-SRB data reflect well the spatial variability of SWD.

[18] Near the GAME-Tibet sites, the standard deviations of the UMD-SRB SWD range over  $10\text{--}15\text{ W m}^{-2}$ , and are

**Table 5.** Mean Bias Errors After Spatial Up-Scaling of UMD-SRB Downward Shortwave Radiation ( $\text{W m}^{-2}$ ) at All the Sites<sup>a</sup>

Resolution	SQH	Gerze	MS3637	Naqu	MS3478	Anduo	D110	TTH	D66	Ave
0.125°	−0.1	−14.5	0.8	12.7	−5.6	9.3	−6.7	−3.1	−0.8	−0.9
1.0°	−11.7	−11.1	15.2	12.5	8.1	7.5	1.9	−8.2	−12.2	0.3
2.5°	−25.7	−10.8	9.6	6.9	2.7	1.8	−5.3	−14.5	−6.9	−4.0

<sup>a</sup>Ave, average values.

comparable to the mean bias errors of GEWEX-SRB and ISCCP-FD (Table 3). Since GEWEX-SRB and ISCCP-FD data represent mean radiation values at coarse-resolution, a question can be raised as to whether the spatial variability of SWD accounts for the mean biases of GEWEX-SRB and ISCCP-FD. To address this issue, both up-scaling and down-scaling methods were used.

[19] The up-scaling method aggregates the UMD-SRB data from fine resolution (0.125°) to coarser resolutions of 1.0° and 2.5° and the results are compared with in situ data. As shown in Table 5, the mean biases at many sites show significant change when the resolution changes from 0.125° to 1.0° or 2.5°, indicating that spatial variability of SWD is important in such a comparison. However, the mean bias averaged over all the sites did not change much, and cannot fully explain the mean biases of ISCCP-FD and GEWEX-SRB in Table 3.

[20] The downscaling method adjusted the satellite data from grid mean to observational site by the following formula before comparison with in situ data:

$$R_{\text{site,gewex}} = \overline{R_{\text{gewex}}} + (R_{\text{site,umd}} - \overline{R_{\text{umd},1.0}}) \quad (1a)$$

$$R_{\text{site,iscsp}} = \overline{R_{\text{iscsp}}} + (R_{\text{site,umd}} - \overline{R_{\text{umd},2.5}}) \quad (1b)$$

where  $\overline{R_{\text{gewex}}}$  and  $\overline{R_{\text{iscsp}}}$  are the GEWEX-SRB and ISCCP-FD SWD grid-means.  $R_{\text{site,gewex}}$  and  $R_{\text{site,iscsp}}$  are the SWD corrected from grids to the observational sites.  $\overline{R_{\text{site,umd}}}$  is the UMD-SRB SWD at the grid nearest to the observational site.  $\overline{R_{\text{umd},1.0}}$  and  $\overline{R_{\text{umd},2.5}}$  are the mean value of UMD-SRB SWD in a 1.0° grid and a 2.5° grid, respectively.

[21] The comparison between the corrected satellite products and in situ data are shown in Table 6. The mean bias decrease by  $4 \text{ W m}^{-2}$  in the ISCCP-FD product and increased somewhat in the GEWEX-SRB product. Again, this indicates that the spatial variability of the SWD cannot fully explain the differences between the GEWEX-SRB and ISCCP-FD with the ground observations.

## 5. Discrepancies Among Satellite Products

[22] It was shown in section 3 that the GEWEX-SRB and ISCCP-FD products underestimate SWD at all the sites. Yet

it is not obvious that this is the case over the entire plateau. Therefore, as a first step, investigated are differences between the satellite products over the entire plateau.

### 5.1. Comparisons of Full-Sky Radiation

[23] We use the UMD-SRB product as a reference and calculate the difference between UMD-SRB and GEWEX-SRB V2.5, V2.81, GEWEX-QCSW V2.5, and ISCCP-FD. GEWEX-SRB V 2.5 shows systematically lower values than UMD-SRB throughout the Plateau (not shown). GEWEX-SRB V2.81 shows a pattern similar to GEWEX-SRB V2.5, but it is much closer to UMD-SRB over most of the Plateau (Figure 4a). The patterns of GEWEX-QCSW V2.5 and ISCCP-FD are more complex, showing higher values in the central part of the plateau (approximately 30–35°N and 80–100°E) and lower values in other parts, as indicated in Figures 4b–4c. This suggests that the errors of satellite products are regionally dependent over the Tibet and it is important to check the spatially distributed discrepancies among different products rather than only the errors for the observational sites.

[24] Interestingly, Figure 4 shows that the discrepancies are usually small for regions with small terrain variability (Figure 3b) while they become much larger for regions with large terrain variability (such as the Himalayas). This suggests that there is a need for additional research on estimating shortwave radiative fluxes in complex terrain. A recent work by Liou *et al.* [2007] has presented the importance of considering radiative transfer processes induced by complex terrain such as the Tibet region.

### 5.2. Comparisons of Clear-Sky Radiation and Cloud Effects

[25] The GEWEX-SRB, QCSW, and ISCCP also produce clear-sky radiation. Figure 5 shows the discrepancies between ISCCP-FD and GEWEX-SRB V2.81 (ISCCP-GEWEX) in clear-sky radiation (panel a), cloud effects (defined as the clear-sky radiation minus full-sky radiation) (panel b), and full-sky radiation (panel c) for July–September, 1998. Surprisingly, the discrepancy in clear-sky radiation is much higher than that in full-sky radiation. The ISCCP-FD generally has higher clear-sky radiation and cloud effects than GEWEX-SRB V2.81 does; and the difference in full-sky radiation is less than that in clear-sky radiation and

**Table 6.** Mean Bias Errors After Spatial Downscaling of GEWEX-SRB V2.81 and ISCCP-FD Data With UMD-SRB Downward Shortwave Radiation ( $\text{W m}^{-2}$ )<sup>a</sup>

Site	SQH	Gerze	MS3637	Naqu	MS3478	Anduo	D110	TTH	D66	Ave
UMD-SRB 0.125°	−0.1	−14.5	0.8	12.7	−5.6	9.3	−6.7	−3.1	−0.8	−0.9
Corrected GEWEX-SRB V2.81	1.4	−16.6	−27.2	−15.3	−32.8	−4.5	−18.0	−27.0	−18.1	−17.6
Corrected ISCCP-FD	13.7	−20.4	−18.4	−6.3	−24.1	−9.6	−5.2	1.5	−4.2	−8.1

<sup>a</sup>Ave, average values.

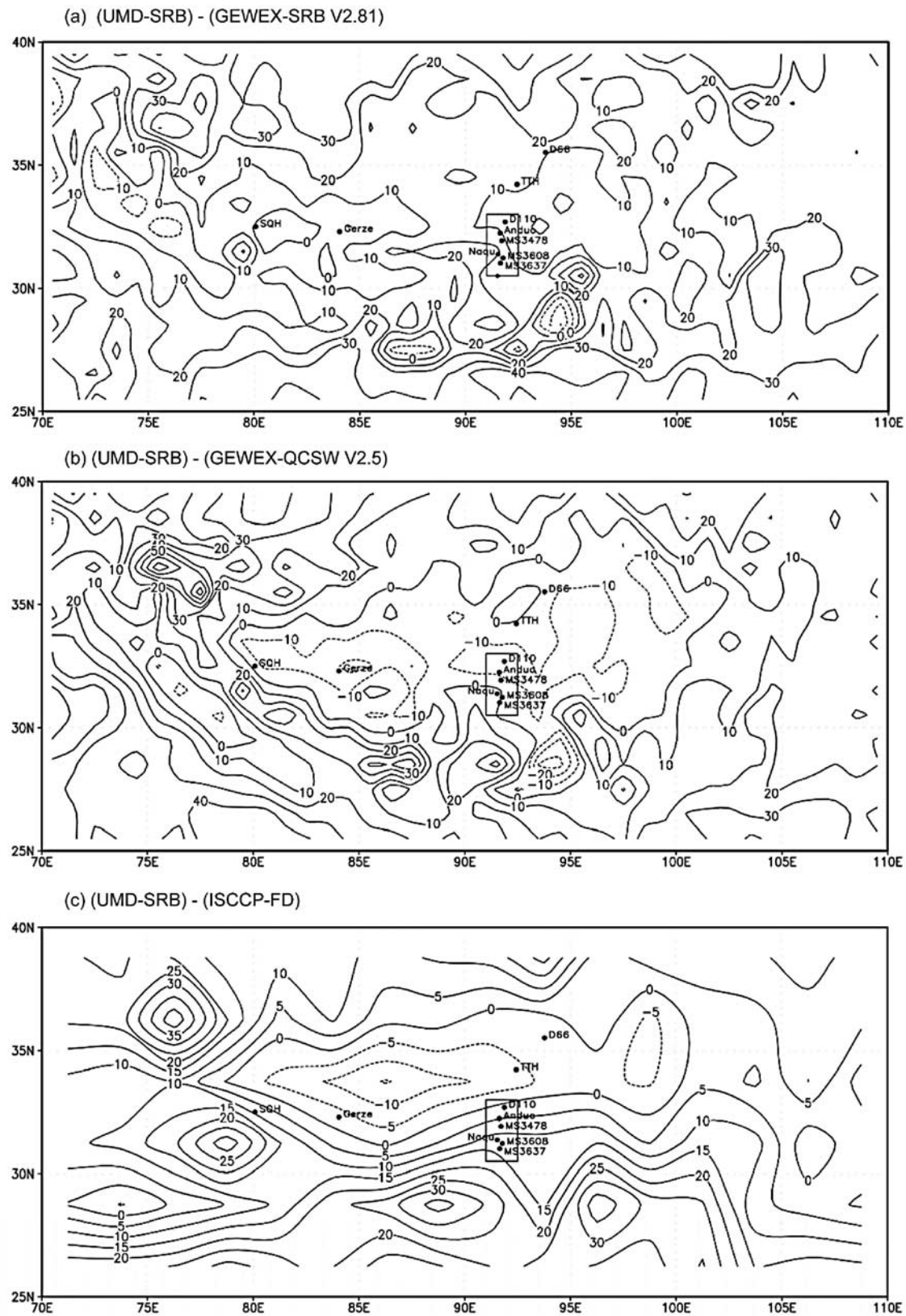


**Figure 4.** Discrepancies of 3 months (July–September 1998) mean SWD among satellite products (UMD-SRB minus other products) over Tibet. UMD-SRB spatial resolution was reduced from  $0.125^\circ$  to  $1.0^\circ$  in panel (a) and (b) and to  $2.5^\circ$  in panel (c). The temporal resolution of the GEWEX-QCSW flux record is truncated to daily, but those fluxes were computed with the 3-hourly satellite data used by GEWEX-SRB.

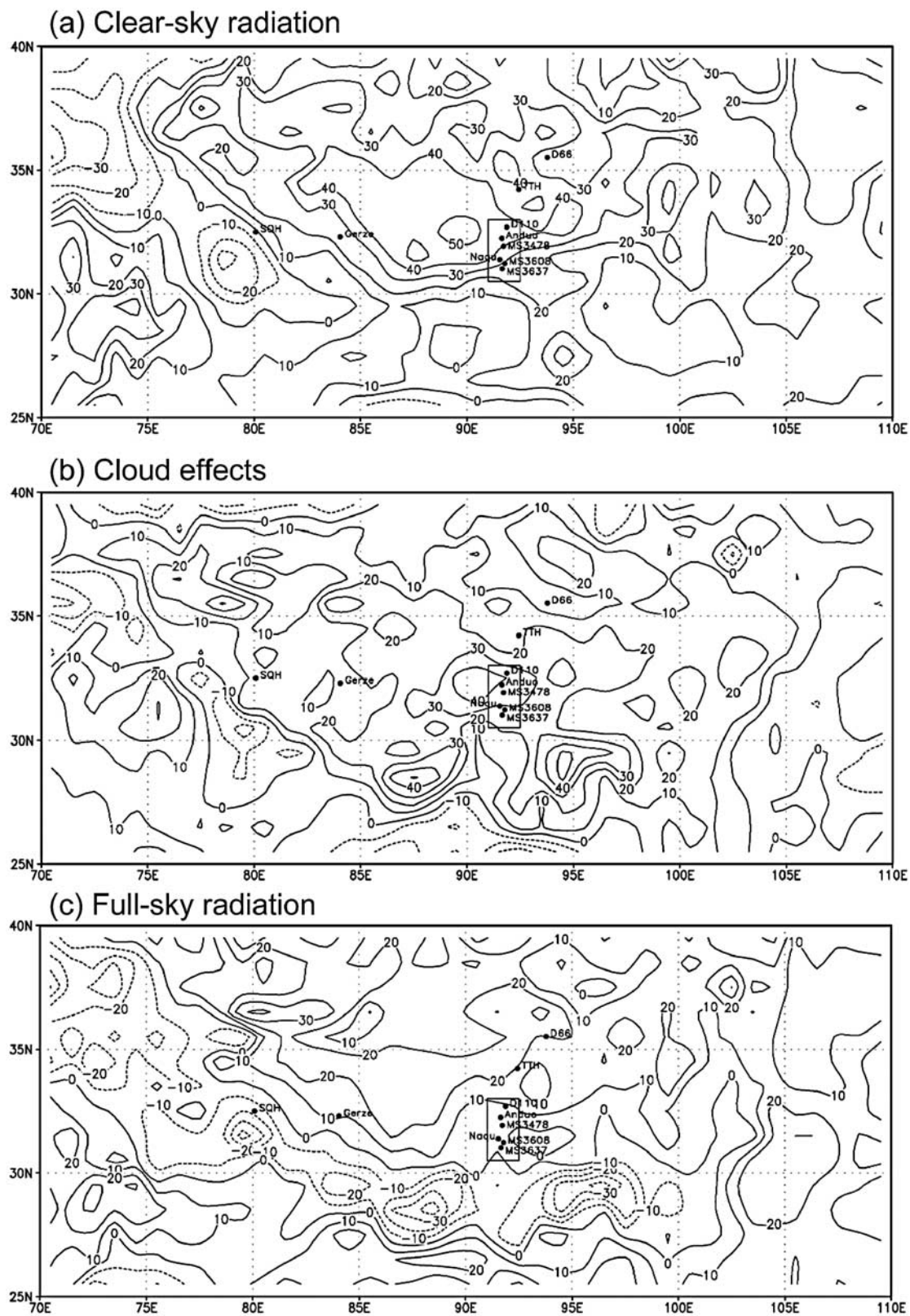


**Figure 5.** The differences of clear-sky radiation, cloud effect, and full-sky radiation between ISCCP-FD and GEWEX-SRB V2.81 (ISCCP-GEWEX), averaged over July–September 1998.

cloud effects due to the partial compensation of the latter two. Similar results are found for the discrepancies between ISCCP-FD and GEWEX-QCSW.

[26] The differences between ISCCP-FD and GEWEX-SRB V2.81 under clear-sky radiation can be attributed to differences in input data, in addition to differences in models. Both GEWEX-SRB and ISCCP-FD used ozone data from the Total Ozone Mapping Spectrometer (TOMS) archives, however, atmospheric profiles of temperature, humidity, and aerosols are different. GEWEX-SRB model uses temperature and humidity profiles from the GEOS-1 reanalysis product of the Global Modeling and Assimilation Office at NASA/Goddard Space Flight Center, and four atmospheric aerosol profiles (MAR-I, MAR-II, CONT-I and CONT-II) of the Standard Radiation Atmosphere (SRA) [see detail in *Pinker and Laszlo*, 1992]. ISCCP-FD uses temperature and humidity profiles from TOVS filled with SAGE temperature climatology and with Oort/SAGE humidity climatology; aerosols are based on the GISS model climatological vertical profiles [*Zhang et al.*, 2004]. As the plateau is a region where most meteorological models show low predictive skill, the larger clear-sky radiation differences in the Plateau (Figure 5a) might imply larger discrepancies in the atmospheric input data. In order to pinpoint the primary source of the differences, there is a need for a future detailed evaluation of this aspect of the study.

## 6. Concluding Remarks

[27] In this study evaluated are four satellite products of downward shortwave radiation (GEWEX-SRB V2.5, GEWEX-SRB V2.81, ISCCP-FD, and UMD-SRB) in the elevated Tibetan Plateau using GAME-Tibet in situ data and the discrepancies among some products (GEWEX-SRB V2.5, GEWEX-SRB V2.81, GEWEX-SRB QCSW V2.5, ISCCP-FD, and UMD-SRB) over the entire plateau.

[28] General underestimations for daily-mean shortwave radiation are found for the GEWEX-SRB V2.5 ( $\sim -49.2 \text{ W m}^{-2}$ ), GEWEX-SRB V2.81 ( $\sim -16.5 \text{ W m}^{-2}$ ), and ISCCP-FD ( $\sim -11.9 \text{ W m}^{-2}$ ) products while the higher resolution UMD-SRB values are closer to GAME-Tibet observations. The difference between GEWEX-SRB V2.5 and GEWEX-SRB V2.81 (about  $30 \text{ W m}^{-2}$ ) shows the need for accounting for the effect of the high elevation in the Tibet, which was neglected unintentionally in GEWEX-SRB V2.5. While, both GEWEX-SRB V2.81 and ISCCP-FD account for altitudinal effects, they still underestimated SWD. The spatial variability of SWD derived from the high-resolution UMD-SRB data cannot fully account for the negative biases in GEWEX-SRB V2.81 and ISCCP-FD.

[29] The satellite data of full-sky radiation, clear-sky radiation and cloud effect were compared over the entire plateau, indicating large discrepancies in all the three parameters. The discrepancies in full-sky radiation are larger for highly variable terrain as compared to relatively simple surfaces. This would suggest that the errors of the satellite products are spatially dependent over the Tibet. While ISCCP-FD product underestimates SWD at all the sites, it should not be implied that it systematically underestimates the radiation throughout the plateau. Yet the errors of satellite products of a coarse resolution increase with terrain complexity. Therefore researchers should take both

elevation and its variability into account when developing coarse-resolution satellite products. Because of the regional dependence of errors of coarse-resolution satellite products and the representativeness of in situ data for complex terrain, it is probably better to evaluate a coarse-resolution product by comparisons with a validated high-resolution product instead of direct comparisons with limited observations.

[30] In addition to the differences in the treatment of elevation and terrain complexity in the satellite inference schemes, differences in model inputs (cloud properties, aerosols, ozone, and humidity profiles), calibration as well as the resolution of the satellite observations may cause discrepancies among satellite products. For instance, GEWEX SRB uses the ISCCP DX pixel level data, which are 4–8 km pixels subsampled at 30 km every 3 hours and averages the pixel radiances to a  $1^\circ \times 1^\circ$  grid. On the other hand, UMD-SRB uses METEOSAT-5 5-km pixels without sampling. Moreover, even with the same model and same satellite inputs but different implementation (e.g., different gap filling or pixel averaging), mentioned is the fact that one can lead to different results. Such issues need also to be addressed in future studies. In addition, in situ data of aerosols, ozone, and humidity profiles over this elevated region should be collected to evaluate their accuracy in satellite models, as the discrepancies in clear-sky radiation are even larger than that in full-sky radiation, e.g., clear-sky radiation of GEWEX-SRB V2.81 is about  $20\text{--}40 \text{ W m}^{-2}$  lower than ISCCP-FD.

[31] Finally, we would like to point out that evaluation of satellite estimates in a complex terrain like the Tibetan Plateau is important and should be pursued as has been done by *Tsuang et al.* [2008] and *Zhou et al.* [2007]. Two ongoing long-term observational networks operational under the Tibet Observation and Research Project (TORP) and the China–Japan Weather Disaster Project, cover a wider Plateau area and are more comprehensive than previous experiments. These observations would be instrumental in the assessment of satellite products and model outputs of radiation, precipitation, precipitable water as well as other hydrometeorological parameters.

[32] **Acknowledgments.** This work was supported by the “Hundred Talent” Project of Chinese Academy of Sciences. The in situ data used in this paper were obtained under the GAME/Tibet project, which was supported by the MEXT, FRSGC, NASDA of Japan, Chinese Academy of Science, and Asian Pacific Network. GEWEX/SRB data were obtained from the NASA Langley Research Center Atmospheric Science Data Center. The work to produce the high resolution radiative fluxes was supported under NASA grant NNG05GB35G to the University of Maryland and benefited from support under NASA grant NNG04GD65G. The authors wish to thank Yves Govaerts and the staff at the European Organization for the Exploitation of Meteorological Satellites (EUMETSAT) Archive and Retrieval Facility for providing the Meteosat-5 observations and consulting on the calibration. Thanks are also due to the National Snow and Ice Data Center (NSIDC) at the University of Colorado, Boulder, CO, for providing the IMS snow data, and to the NOAA-CIRES Climate Diagnostic Center for providing the NCEP Reanalysis II data.

## References

- Chen, L. X., F. Schmidt, and W. Li (2003), Characteristics of the atmospheric heat source and moisture sink over the Qinghai–Tibetan Plateau during the second TIPEX of summer 1998 and their impact on surrounding monsoon, *Meteorol. Atmos. Phys.*, **83**, 1–18.
- Cox, S. J., P. W. Stackhouse Jr., S. K. Gupta, J. C. Mikovitz, T. Zhang, L. M. Hinkelman, M. Wild, and A. Ohmura (2006), The NASA/GEWEX Surface Radiation Budget Project: Overview and Analysis, in 12th Conference on Atmospheric Radiation, Madison, Wis., 10–14 July.

- Dutton, E. G., J. J. Michalsky, T. Stoffel, B. W. Forgan, J. Hickey, D. W. Nelson, T. L. Alberta, and I. Reda (2001), Measurement of broadband diffuse solar irradiance using current commercial instrumentation with a correction for thermal offset errors, *J. Atmos. Ocean. Technol.*, **18**, 297–314.
- Flohn, H. (1957), Large-scale aspects of the “summer monsoon” in South and East Asia, *J. Meteorol. Soc. Jpn.*, **35**, 180–186.
- Gupta, S. K., D. P. Kratz, P. W. Stackhouse Jr., and A. C. Wilber (2001), *The Langley Parameterized Shortwave Algorithm for Surface Radiation Budget Studies (Vers. 1.0)*, NASA/TP-2001-211272, 31 pp. (Available online at <http://techreports.larc.nasa.gov/ltrs/ltrs.html>)
- Kato, S., T. P. Ackerman, E. E. Clothiaux, J. H. Mather, G. R. Mace, M. Wesley, F. Murcray, and J. Michalsky (1997), Uncertainties in modeled and measured clear-sky surface shortwave irradiances, *J. Geophys. Res.*, **102**, 25,881–25,898.
- Koike, T. (2004), The coordinated enhanced observing period—an initial step for integrated global water cycle observation, *WMO Bull.*, **53**(2), 1–8.
- Koike, T., T. Yasunari, J. Wang, and T. Yao (1999), GAME-Tibet IOP summary report, in *Proc. of the 1st Int'l Workshop on GAME-Tibet, January 11–13, 1999*, pp. 1–2, Xi'an, China.
- Kurosaki, Y., and F. Kimura (2002), Relationship between topography and daytime cloud activity around Tibetan Plateau, *J. Meteorol. Soc. Jpn.*, **80**, 1139–1155.
- Kuwagata, T., A. Numaguti, and N. Endo (2001), Diurnal variation of water vapor over the central Tibetan Plateau during summer, *J. Meteorol. Soc. Jpn.*, **79**(1B), 401–418.
- Li, Z., C. H. Whitlock, and T. P. Charlock (1995), Assessment of the global monthly mean surface insolation estimated from satellite measurements using global energy balance archive data, *J. Clim.*, **8**, 315–328.
- Li, X., R. T. Pinker, M. M. Wonsick, and Y. Ma (2007), Towards improved satellite estimates of short-wave radiative fluxes: Focus on cloud detection over snow: 1. Methodology, *J. Geophys. Res.*, **112**, D07208, doi:10.1029/2005JD006698.
- Liou, K. N., W.-L. Lee, and A. Hall (2007), Radiative transfer in mountains: Application to the Tibetan Plateau, *Geophys. Res. Lett.*, **34**, L23809, doi:10.1029/2007GL031762.
- Liu, H., and R. T. Pinker (2008), Radiative fluxes from satellites: Focus on aerosols, *J. Geophys. Res.*, **113**, D08208, doi:10.1029/2007JD008736.
- Liu, H., R. T. Pinker, and B. N. Holben (2005), A global view of aerosols from merged transport models, satellite, and ground observations, *J. Geophys. Res.*, **110**, D10S15, doi:10.1029/2004JD004695.
- Liu, J., J. A. Curry, W. B. Rossow, J. R. Key, and X. Wang (2005), Comparison of surface radiative flux data sets over the Arctic Ocean, *J. Geophys. Res.*, **110**, C02015, doi:10.1029/2004JC002381.
- Ma, Y., S. Fan, H. Ishikawa, O. Tsukamoto, T. Yao, T. Koike, H. Zuo, Z. Hu, and Z. Su (2005), Diurnal and inter-monthly variation of land surface heat fluxes over the central Tibetan Plateau area, *Theor. Appl. Climatol.*, **80**, 259–273.
- Ma, Y., M. Song, H. Ishikawa, K. Yang, T. Koike, L. Jia, M. Meneti, and Z. Su (2007), Estimation of the regional evaporative fraction over the Tibetan Plateau area by using Landsat-7 ETM data and the field observations, *J. Meteorol. Soc. Jpn.*, **85A**, 295–309.
- Ma, Y.-T., R. T. Pinker, B. Zhang, Y.-C. Zhang, and W. B. Rossow (2007), Comparison of UMD/SRB V3.1 ISCCP D1 fluxes with those of ISCCP-FD: Source of differences, GEWEX Radiative Flux Assessment, Third Workshop, NASA GISS, New York, 25–27 June.
- Pinker, R. T., and I. Laszlo (1992), Modeling surface solar irradiance for satellite applications on a global scale, *J. Appl. Meteor.*, **31**, 194–211.
- Pinker, R. T., et al. (2003), Surface radiation budgets in support of the GEWEX Continental Scale International Project (GCIP) and the GEWEX Americas Prediction Project (GAPP), including the North American Land Data Assimilation System (NLDAS) project, *J. Geophys. Res.*, **108**(D22), 8844, doi:10.1029/2002JD003301.
- Ramanathan, V., P. J. Crutzen, J. Lelieveld, D. Althausen, J. Anderson, M. O. Andreae, W. Cantrell, G. Cass, and C. E. Chung (2001), The Indian Ocean Experiment: An integrated assessment of the climate forcing and effects of the great Indo-Asian haze, *J. Geophys. Res.*, **106**, 28,371–28,398.
- Ramsay, B. (1998), The interactive multi-sensor snow and ice mapping system, *Hydrol. Process.*, **12**, 1537–1546.
- Raschke, E., S. Bakan, and S. Kinne (2006), An assessment of radiation budget data provided by the ISCCP and GEWEX-SRB, *Geophys. Res. Lett.*, **33**, L07812, doi:10.1029/2005GL025503.
- Rossow, W. B., and R. Schiffer (1999), Advances in understanding clouds from ISCCP, *Bull. Am. Meteorol. Soc.*, **80**, 2261–2287.
- Stackhouse, P. W., S. K. Gupta, S. J. Cox, J. C. Mikovitz, T. Zhang, and M. Chiacchio (2004), 12-year surface radiation budget data set, *GEWEX News*, **14**, 10–12.
- Tsuang, B.-J., M.-D. Chou, Y. Zhang, A. Roesch, and K. Yang (2008), Evaluations of land/ocean skin temperatures of the ISCCP satellite retrievals and the NCEP and ERA reanalyses, *J. Clim.*, **21**, 308–330.
- Wu, G., Y. Liu, T. Wang, R. Wan, X. Liu, W. Li, Z. Wang, Q. Zhang, A. Duan, and X. Liang (2007), The influence of mechanical and thermal forcing by the Tibetan Plateau on Asian climate, *J. Hydrometeorol.*, **8**, 770–789.
- Xia, X. A., P. C. Wang, H. B. Chen, and F. Liang (2006), Analysis of downwelling surface downward shortwave radiation in China from National Centers for Environmental Prediction reanalysis, satellite estimates, and surface observations, *J. Geophys. Res.*, **111**, D09103, doi:10.1029/2005JD006405.
- Yanai, M., C. Li, and Z. Song (1992), Seasonal heating of the Tibetan Plateau and its effects on the evolution of the Asian summer monsoon, *J. Meteorol. Soc. Jpn.*, **70**, 319–351.
- Yang, K., T. Koike, P. Stackhouse, C. Mikovitz, and S. J. Cox (2006a), An assessment of satellite surface radiation products for highlands with Tibet instrumental data, *Geophys. Res. Lett.*, **33**, L22403, doi:10.1029/2006GL027640.
- Yang, K., T. Koike, and B. Ye (2006b), Improving estimation of hourly, daily, and monthly downward shortwave radiation by importing global data sets, *Agric. Forest. Meteorol.*, **137**, 43–55.
- Yang, K., T. Watanabe, T. Koike, X. Li, H. Fujii, K. Tamagawa, Y. Ma, and H. Ishikawa (2007), Auto-calibration system developed to assimilate AMSR-E data into a land surface model for estimating the soil moisture and surface energy budget, *J. Meteorol. Soc. Jpn.*, **85A**, 229–242.
- Yeh, T. C., and Y. X. Gao (1979), *The Meteorology of the Qinghai-Xizang (Tibet) Plateau*, 278 pp., Science Press, Beijing.
- Yeh, T. C., S.-W. Lo, and P.-C. Chu (1957), The wind structure and heat balance in the lower troposphere over Tibetan Plateau and its surroundings, *Acta Meteorol. Sin.*, **28**, 108–121.
- Zhang, Y.-C., W. B. Rossow, and A. A. Lacis (1995), Calculation of surface and top of atmosphere radiative fluxes from physical quantities based on ISCCP data sets: 1. Method and sensitivity to input data uncertainties, *J. Geophys. Res.*, **100**, 1149–1165.
- Zhang, Y.-C., W. B. Rossow, A. A. Lacis, V. Oinas, and M. I. Mishchenko (2004), Calculation of radiative fluxes from the surface to top of atmosphere based on ISCCP and other global data sets: Refinements of the radiative transfer model and the input data, *J. Geophys. Res.*, **109**, D19105, doi:10.1029/2003JD004457.
- Zhou, Y., D. P. Kratz, A. C. Wilber, S. K. Gupta, and R. D. Cess (2007), An improved algorithm for retrieving surface downwelling longwave radiation from satellite measurements, *J. Geophys. Res.*, **112**, D15102, doi:10.1029/2006JD008159.

S. J. Cox, Analytical Services and Materials, Inc., One Enterprise Parkway, Suite 300, Hampton, VA 23666, USA.

T. Koike, Department of Civil Engineering, University of Tokyo, Hongo 7-3-1, Bunkyo-ku, Tokyo 113-8656, Japan.

Y. Ma and K. Yang, Institute of Tibetan Plateau Research, Chinese Academy of Sciences, P.O. Box 2871, Beijing 100085, China. (yangk@itpcas.ac.cn)

R. T. Pinker and M. M. Wonsick, Department of Atmospheric and Oceanic Science, University of Maryland, Space Sciences Building, College Park, MD 20742, USA.

P. Stackhouse, NASA Langley Research Center, 21 Langley Boulevard, M.S. 420, Hampton, VA 23681, USA.

Y. Zhang, Columbia University at NASA GISS, 2880 Broadway, Room 320-B, New York, NY 10025, USA.